Derivation of a new continuous adjustment function for correcting wind-induced loss of solid precipitation: results of a Norwegian field study

M. A. Wolff[1], **K. Isaksen**[1], **A. Petersen-Øverleir**[2], **K. Ødemark**[1], **T. Reitan**[3], **and R. Brækkan**[1]

[1]Norwegian Meteorological Institute, Oslo, Norway
[2]Statkraft, Oslo, Norway
[3]Norwegian Water Resources and Energy Directorate, Oslo, Norway

Correspondence to: M. A. Wolff (mareilew@met.no)

Abstract. Precipitation measurements exhibit large cold-season biases due to under-catch in windy conditions. These uncertainties affect water balance calculations, snowpack monitoring and calibration of remote sensing algorithms and land surface models. More accurate data would improve the ability to predict future changes in water resources and mountain hazards in snow-dominated regions.

In 2010, a comprehensive test site for precipitation measurements was established on a mountain plateau in southern Norway. Automatic precipitation gauge data are compared with data from a precipitation gauge in a Double Fence Intercomparison Reference (DFIR) wind shield construction which serves as the reference. A large number of other sensors are provided supporting data for relevant meteorological parameters.

In this paper, data from three winters are used to study and determine the wind-induced under-catch of solid precipitation. Qualitative analyses and Bayesian statistics are used to evaluate and objectively choose the model that best describes the data. A continuous adjustment function and its uncertainty are derived for measurements of all types of winter precipitation (from rain to dry snow). A regression analysis does not reveal any significant misspecifications for the adjustment function, but shows that the chosen model does not describe the regression noise optimally. The adjustment function is operationally usable because it is based only on data available at standard automatic weather stations.

The results show a non-linear relationship between under-catch and wind speed during winter precipitation events and there is a clear temperature dependency, mainly reflecting the precipitation type. The results allow, for the first time, derivation of an adjustment function based on measurements above $7\,\mathrm{m\,s^{-1}}$. This extended validity of the adjustment function shows a stabilization of the wind-induced precipitation loss for higher wind speeds.

1 Introduction

In addition to rising global temperatures, climate models also predict significant changes to the hydrological cycle. Water and the availability of water are indispensable to life. More than one-sixth of Earth's population gets most of their water supply from glaciers and seasonal snow packs and many of these are in jeopardy (Barnett et al., 2005). Precipitation observations are important for describing the hydrological cycle quantitatively. Their accuracy needs to be improved further to allow for a better evaluation and verification of numerical weather forecast, hydrological and climate models and thereby enhance these models' capabilities to predict short- and long-term changes as well as the variability of the world's water budget with greater confidence (Seneviratne et al., 2012).

It has been known for a long time that especially measuring precipitation in the form of snow is difficult. The fact that wind induces a bias on solid precipitation measurements is well established. For example, Brown and Peck (1962) addressed the challenges of precipitation measurements re-

lated to exposure in 1962. This systematic under-catch can be somewhat reduced by shielding the gauge, and various types of windshield configurations have been developed for this purpose (e.g. Alter, Tretyakov). However, even with a windshield applied, a wind bias still remains evident in snow measurements and requires an adjustment. In the 1980s, methods for correcting systematic errors in precipitation measurements for operational use were suggested, as described in Sevruk (1982).

The most recent comprehensive study of the problem was organized by the WMO Solid Precipitation Intercomparison Committee between 1987 and 1993 (Goodison et al., 1998). One outcome of that study is the recommendation of the Double Fence Intercomparison Reference (DFIR) as the reference snow measurement. The study assessed and derived adjustment functions for solid precipitation measurement configurations used at that time, which to a large extent are manual observations.

Førland et al. (1996) developed and described a more operational method for correcting precipitation measurements in the Nordic countries based on the findings of the Jokioinen test site in Finland, as described in Goodison et al. (1998). This method, or variations on it (e.g. Hanssen-Bauer et al., 1996), are in wide use by Norway's hydropower companies whose budget calculations depend on accurate precipitation measurements.

Another large-scale application of the adjustment functions from Goodison et al. (1998) for daily observations of Nordic precipitation stations (north of 45° N) across national boundaries is performed by Yang et al. (2005). The applied bias corrections enhanced monthly precipitation amounts by 5–20 %, depending on the season and the local climate. Yang et al. (2005) suggested reviewing the current understanding of the Arctic fresh water budget and its change based on their findings.

Førland and Hanssen-Bauer (2000) analysed and adjusted precipitation measurements at Svalbard. Temperatures are rising significantly in the Arctic, altering the annual distribution of solid and liquid precipitation events. Today, a higher percentage of the annual precipitation is falling as rain. This results in a fictitious increase of precipitation amount, as rain is less affected by the wind-induced bias than snow. Førland and Hanssen-Bauer (2000) show that this artifactual increase of precipitation amount is of a similar magnitude as the expected real increase of precipitation amount due to climate change.

Rasmussen et al. (2012) present recent efforts to understand the relative accuracies of different instrumentation, gauges and windshield configurations to measure snowfall that have been developed since the WMO Intercomparison Test of Solid Precipitation (1989–1993), at the National Center for Atmospheric Research (NCAR) Marshall Field Site.

In recent years, an increasing number of stations are automated. However, information regarding measurement uncertainty for automatic measurements is lacking. While there are several studies on measurements of solid precipitation, only a few focus on the accuracy of automatic precipitation measurements (Rasmussen et al., 2012). This problem is also given attention in the IPCC AR5 (Bindoff et al., 2013) which states that observational uncertainties, in addition to challenges in precipitation modelling, limit confidence in the assessment of climatic changes in precipitation.

From 2008 to 2009, the performance of a large number of precipitation gauges and windshield configurations is evaluated against a DFIR at Environment Canada's CARE and Bratt's Lake sites (Smith and Yang, 2010; Rasmussen et al., 2012). A survey is conducted by Nitu and Wong (2010) to develop a summary of current methods and instruments for measuring solid precipitation. They found that the variation in gauges and windshield configurations is much larger for automatic stations than for manual stations. The results indicated further that a review of the current state-of-the-art methodologies is required to increase the precipitation measurement accuracy. Following that, the Commission for Instruments and Methods of Observations (CIMO) within WMO took on a leadership role for evaluating gauges for solid precipitation measurements in cold and Alpine climates within the WMO-CIMO Solid Precipitation Intercomparison Experiment (WMO-SPICE). WMO-SPICE is a multi-site effort with 20 host sites worldwide. A wide range of today's automated precipitation gauges and configurations are evaluated at these sites. More information about SPICE can be found on the SPICE website: http://www.wmo.int/pages/prog/www/IMOP/intercomparisons/SPICE/SPICE.html.

This paper presents the results from the Norwegian test site located on a mountain plateau in southern Norway. The site was established in 2010, as an initiative by Norway's hydropower companies in need of accurate snow measurements for predicting water resources. Besides its original purpose, the site also became a host site for WMO SPICE in 2013 and will continue operating as a long-term reference station for monitoring changes in precipitation amount in Norway. The station is also part of a newly established national network for improved avalanche forecasting.

The objective of this study is to determine the wind-induced under-catch of solid precipitation and develop a continuous adjustment function for measurements of all types of winter precipitation (from rain to dry snow), which can be used for operational measurements based on data available at standard automatic weather stations. Qualitative analyses and Bayesian statistics are used to evaluate and objectively choose the model best describing the data.

The chosen locality has proven to be ideal for this purpose. The site receives a lot of snow, often accompanied by high winds, which provides many events suitable for studying the wind influence on solid precipitation. The high wind speeds encountered contribute to making a unique data set when compared to other test sites, where such strong winds are less common.

The measurement site and its climate are described in Sect. 2. Section 3 describes the data preparation performed in advance of the main analysis, as well as the analysis methods used. Results are presented in Sect. 4, followed by a discussion and conclusions in Sects. 5 and 6, respectively.

2 Measurement site

2.1 Site description

Haukeliseter test site is situated on a mountain plateau in southern Norway (59.82° N and 7.21° E at 991 m a.s.l.), see Fig. 1. All instruments are placed on a 5000 m² flat area, surrounded by topographic variations up to 20 m in the immediate vicinity and then slowly increasing to the surrounding mountain tops which are between 100 and 500 m higher.

The area is situated between two lakes and the closest mountaintop (distance 1 km) has an altitude of 1162 m a.s.l., located towards the northeast. The mountains to the east are ca. 1250 m a.s.l. at a distance of 2 km. The terrain is more open towards the south and the west, with mountains 4 and 3 km away, respectively.

Precipitation sensors are mounted side by side perpendicular to the prevailing wind from easterly and westerly directions in order to minimize mutual disturbances. The reference configuration at Haukeliseter consists of an automatic precipitation gauge (Geonor T200-BM, 1000 mm, 3 transducers; Geonor AS, Norway) and an Alter wind shield, both centred in an octagonal double fence (DF) construction that effectively minimizes the wind-influence on the precipitation measurements. The DF is similar to the Double Fence Intercomparison Reference (DFIR) of the first WMO intercomparison (Goodison et al., 1998) where it is used with a Tretyakov manual gauge. The combination of the DF and the automated gauge at Haukeliseter also fulfils the specifications for the official DFAR (Double Fence Automated Reference) of the ongoing WMO-SPICE (WMO/CIMO, 2012).

Additionally, measurements of numerous other meteorological parameters are performed to support the analysis of the precipitation data. Air temperature is measured with a pt100 element (1/10 DIN) protected by a standard Norwegian radiation screen, installed at gauge height on a tower close to the DFIR.

Wind is measured by different sensors at several places around the measurement site. Standard 10 m wind measurements are performed at the tower close to the DFIR with an ultrasonic wind sensor from Gill (Windobserver II with extended heating). Three wind sensors are directly mounted to the precipitation gauges for measuring wind at gauge height (Windobserver II at precipitation gauge inside DFIR, and Young Wind Monitor SE at the two closest precipitation sensors – X1 and X2, see layout). In 2013, a Thies Ultrasonic Wind Anemometer 3-D was installed on a separate mast at

4.5 m (gauge height) to allow measurements undisturbed by the precipitation sensor installations (see Sect. 3.1.2).

Several optical precipitation detectors (Thies precipitation sensor) are placed on the two 10 m masts at the site. In the described event selection, one of these sensors (selected because of its stability over the course of the experiment) is used for the event selection, see Sect. 3.1.1.

Furthermore, one forward scatter instrument (Vaisala PWD 21) and two disdrometer type instruments (Thies LPM and Ott Parsivel) are installed on the meteorological mast close to the DFIR, providing additional information on the precipitation type, see Sect. 3.3.3.

Further information about the test site, including an evaluation of the homogeneity and a list of instruments, can be found in Wolff et al. (2010, 2013).

2.2 Climate

The Haukeliseter test site was chosen because of its significant number of snow events often paired with high wind speeds during the 6 to 7 month-long winters. Solid precipitation is commonly observed between October and May, but can also occur during the summer months. The mean annual air temperature (MAAT, 1961–1990) for the site is 0.6 °C. Mean monthly temperatures are below 0 °C for the period November to April, with an estimated mean air temperature (1961–1990) of −5.4 °C. The estimated, uncorrected annual precipitation (1961–1990) is approximately 800 mm of which more than 50 % is solid precipitation. In a normal winter, the average snow depth reaches approximately 1.5–2.0 m.

Further, 10 years of winter observations from the nearby manual station "Haukeliseter Brøytestasjon" (800 m distance) operating between 1984 and 1995 reported a significant number of snow events with maximum wind speed above 15 m s^{-1}. These observations also contain a frequent occurrence of blowing and drifting snow, a significant number of these below eye-height. The precipitation gauges at Haukeliseter are therefore mounted relatively high – at 4.5 m – in order to minimize the influence of blowing and drifting snow on the measurements.

Data for this study were collected over the course of three winters, from early 2011 until May 2013. Figure 2 shows the monthly precipitation and mean temperature anomaly with respect to the normal period 1961–1990 for all measurement months, based on data from the official nearby meteorological station Vågsli (821 m a.s.l., located 10 km to the east). Months not identified as "measurement months" are used for maintenance and upgrades of the equipment at the test site.

All three months of the first period in 2011 were characterized by a higher precipitation amount than normal. Whereas February 2011 was relatively cold, March and April 2011 were rather warm. April 2011, with a mean temperature of 4.8 °C above the normal monthly mean temperature, was registered as the warmest April since 1900 in large areas of southern Norway.
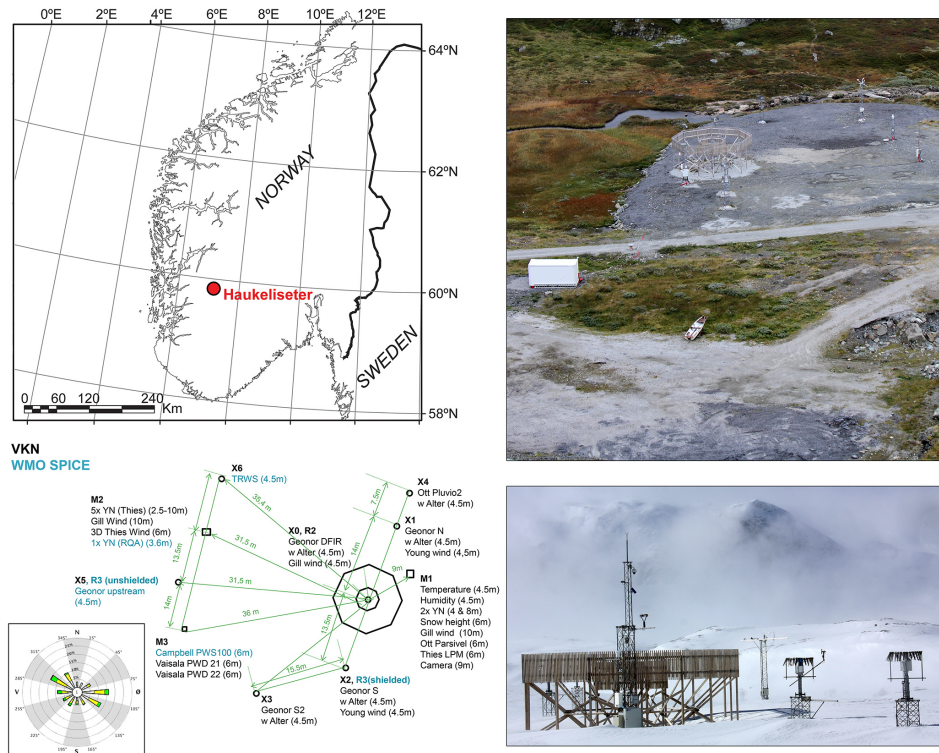
Figure 1. Localization of the test site Haukeliseter in southern Norway (upper left). The lower left panel shows the layout of the site and a wind rose showing the statistical distribution of wind directions. The layout is orientated in the same way as the wind rose. The two photographs show the test site. The picture in the upper right was taken by Ole Jørgen Østby from aboard a helicopter. The picture in the lower right was taken by Roy Rasmussen.

The second winter (November 2011–April 2012) was continuously mild (with the exception of April 2012) and a higher precipitation amount than usual was registered (with the exception of March 2012). In December 2011, more than double of the normal monthly precipitation amount was observed. March 2012 was the warmest March ever recorded in western and eastern Norway. The mean temperature at Vågsli was 6.2 °C above the normal monthly temperature.

The third winter was characterized by low temperatures. Whereas during February and March 2013 very little precipitation occurred, April and May 2013 were characterized by very high precipitation amounts.

3 Data and methods

Measurements from all precipitation instruments and meteorological auxiliary measurements were monitored every minute from two combined data loggers (SM5049 by Scanmatic AS, Norway). Data were transferred hourly to the Norwegian Meteorological Institute (MET Norway) and stored in the official Climate Data Base, assuring long-term storage and availability for data analysis.

At MET Norway, the data of all instruments are manually quality controlled by a data analyst. A more detailed analy-

sis of the wind measurements revealed disturbances caused by the nearby installations. Therefore, selected wind sectors are excluded from the further data analysis (further details in Sect. 3.1.2).

3.1 Data preparation

3.1.1 Precipitation events

An algorithm has been developed to guarantee an objective method for identifying precipitation periods with significant and for the most part continuous accumulation. The algorithm is applied on the complete data set containing 10 min running averages of the measurements by the DF-Geonor and a precipitation detector (Yes/No).

The following thresholds are used to check for (a) continuity and (b) significance of the precipitation periods:

a. 8 out of 10 min must contain registered precipitation (from precipitation detector).

b. Accumulation must be more than 0.1 mm per 10 min or, in the case of event duration longer than 100 min, more than 1 mm for the entire event period.

The resulting precipitation periods are of various lengths and are divided into 10 and 60 min events, respectively, creating
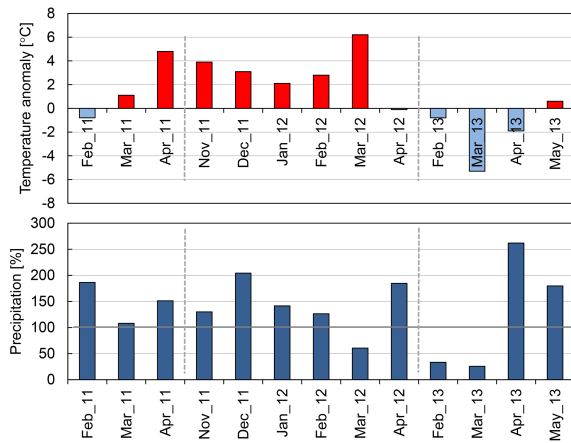
Figure 2. Temperature (top) and precipitation (bottom) anomaly with respect to normal period (1961–1990) at Vågsli, the closest official weather station to Haukeliseter.

two versions of the event data set. The complete event data set contains the identified periods (of either 10 or 60 min duration), accumulation measured in all precipitation gauges, mean and standard deviation of temperature, wind speed, wind direction and humidity, net precipitation time in minutes and typical weather codes as measured from the present weather sensor.

The introduction of thresholds implies that events interrupted by breaks or characterized by a very low accumulation rate are ignored. Furthermore, an event might start and/or end with a lower rate and might therefore not being registered over its full length. The described method, however, guarantees that only unambiguous events are used in the following analysis and thus determine dependencies with higher accuracy.

The qualitative analysis is performed on both 10 and 60 min events, but no significant differences are found. The quantitative analysis is performed on the 60 min events only because that time interval is similar to the operational measurement frequency in Norway.

3.1.2 Wind measurements at 10 m height and gauge height

Wind measurements at the test site are recorded by different sensors, ultrasonic and mechanical (propel), mounted at 10 m (standard height) and gauge height. Before 2013, gauge height wind measurements were solely performed by sensors mounted on the pedestals of the precipitation gauges, placing the wind sensors in the direct vicinity of the wind shields around the gauges. Comparisons with a gauge height wind sensor on a separate mast (installed in 2013) confirm the expected impact of the precipitation gauge and wind shield on the wind measurements of the anemometers mounted near the shield. Wind directions between 0 and 240° are affected.
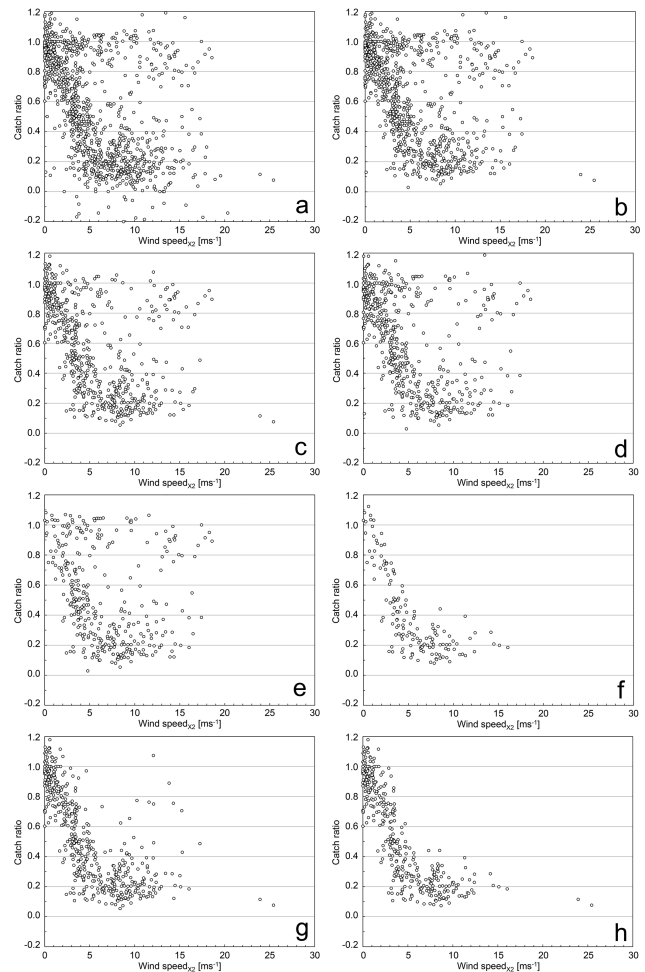

Figure 3. Catch ratio between Geonor South (X2) and DF-Geonor versus wind speed (measured at gauge height). Different filters are applied on all 1-hour precipitation events from three winter seasons (2011–2013). **(a)** All precipitation events without filter. **(b)** Events where the accumulation measured by Geonor South (X2) is larger than 0.1 mm within the last hour. **(c)** An additional filter cuts all events with an average wind direction between 355 and 55°, corresponding to the sector where a shadowing effect of the DFIR construction can be expected. **(d)** An additional filter cuts all events where temperature standard deviation exceeds 0.2 °C. **(e)** Shows only event with additional low wind speed variations. The threshold is set to a maximum of 0.2 for the ratio between standard deviation and mean wind speed. On the data in **(f)** are the same filters applied as for data in **(e)** – only events with mean temperature below −2 °C are shown; **(g)** and **(h)** show data with the same filter applied as in **(c)**, for temperatures lower than 0 °C **(g)** and lower than −2 °C **(h)**.

For the analysis of the gauge height wind data, only precipitation events with wind directions from non-affected sectors are considered. Analysis is also performed with the undisturbed wind data from the 10 m sensor, mounted separately on top of a mast. For these data no filtering is necessary and the analysis is performed with the undisturbed data set. These

two data sets are hereafter referred to as "gauge height wind data set" and "10 m wind data set".

3.2 Data filtering

Catch ratios between standard Geonor configurations and the DF-Geonor for all identified events are calculated. Figure 3 shows the results for the southern Geonor precipitation gauge X2 (see layout in Fig. 1), as this sensor provides the most stable data set. The large amount of scatter visible in panel a (all events), including some very clear outliers, makes it necessary to evaluate the influence of various parameters in more detail.

A few negative catch ratios are visible in panel a, which are mainly due to only small accumulation inside the DF-Geonor and no significant accumulation in the X2-Geonor. For these cases the noise of the transducers dominates the X2-signals. They subsequently vary around zero, thus resulting in negative catch ratios. For panel b an additional threshold is introduced, accepting only events for which the X2-Geonor collected more than 0.1 mm, and thus removing the unrealistic very small or negative catch ratios. About 5 % of the recorded events inside the DF at Haukeliseter show no significant accumulation in the gauges outside.

Since the installations are optimized for minimized influence under prevailing wind directions (installation along a line, see site layout in Fig. 1), shadowing effects on the precipitation measurements are likely for other wind directions. Precipitation measurements by the Geonor X2 will be mostly affected by shadowing for wind directions between 355 and 55°. Panel c shows all events where these wind directions are removed using data from the wind sensor at 10 m height. The resulting data points show a little less scatter for lower wind speeds. The effect is more visible when considering only snow events. Panels g and h are based on the same data as in panel c, but show only data measured at temperatures below 0 °C and below −2 °C, respectively.

Variations of both temperature and wind speed during an event are evaluated. Events with a standard deviation smaller than 0.2 °C during the event period are shown in panel d, although other thresholds are tested (not shown). It seems most natural to weight wind speed variations by the mean wind speed. The maximum ratio between the standard deviation of wind speed and the mean wind speed is set to 0.2 for the events shown in panel e. The same filters are applied in panel f as for panel e, however only events with mean temperature below −2 °C are shown. These latter filter methods for temperature and wind speed variations do not improve the catch ratio data set from Haukeliseter. Removed data points are evenly spread and no significant noise reduction is achieved. Therefore, no thresholds for limiting temperature and wind speed variations are used for the further analysis.
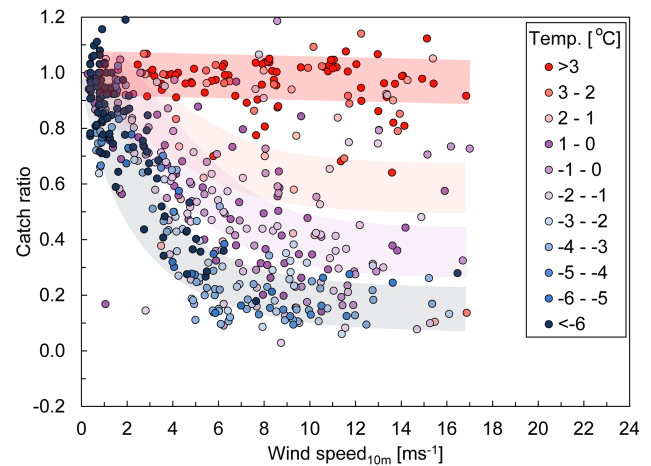

Figure 4. Catch efficiency of the south Geonor (X2) compared to DFIR for different wind speeds (10 m height), classified for temperature (colour coded, see legend). Data are from 2011–2012. Data are filtered: a significant (> 0.1 mm) accumulation at the south Geonor is required; events with possible affected wind directions are neglected. The coloured areas show the continuous temperature-dependent change in the shape of the catch ratio curve.

3.3 Qualitative analysis

In a further step, the data set is analysed qualitatively in order to get a more detailed understanding of how the catch ratio is influenced by various parameters. For this purpose, the data set is divided into classes for temperature, wind, precipitation type and intensity.

3.3.1 Temperature

Figure 4 shows the catch ratio for different temperature classes in 1 K steps. For temperatures above 2 °C, where precipitation is mainly falling as rain, the catch ratio is not influenced significantly by the wind. For temperatures below −2 °C, where precipitation is mainly falling as snow, the catch ratio curve has a characteristic shape, indicating a clear dependence on the wind speed. This relationship does not change significantly for further decreasing temperatures.

For temperatures between 2 and −2 °C, where snow, rain and mixed precipitation can occur, an increased scatter is visible in the data, obviously depending on the precipitation type for each individual event. The four temperature classes in this region, however, still suggest a continuous change from higher to lower temperatures. That is consistent with the expectation of a gradual change of the distribution of liquid and solid precipitation particles during a mixed-phase event.

3.3.2 Wind

Concentrating only on snow data, in order to reduce the scatter due to varying precipitation types, data are divided into wind speed classes. The average catch ratios for stepwise in-
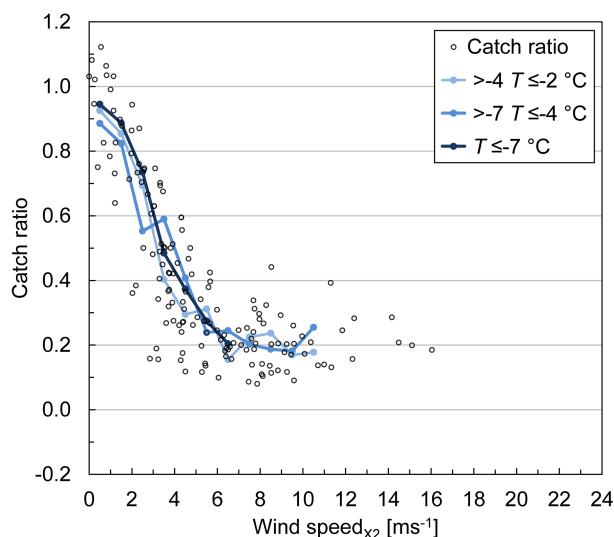
Figure 5. Catch ratio between the south Geonor (X2) and the DFIR-Geonor versus wind speed. Only temperature classes where precipitation is expected as snow are shown. The overlaid curves show data collected into $1\,\mathrm{m\,s^{-1}}$ wind speed classes. Data from 2011–2013 are shown and filtered according to the description of panel **(c)** in Fig. 3.

creasing wind speed classes are shown in Fig. 5 and suggest a non-linear dependence on the wind speed. After a steep slope with increasing wind, the catch ratio seems to stabilize around 20 % for wind speeds higher than $7\text{–}8\,\mathrm{m\,s^{-1}}$. No obvious temperature dependence for these lower temperature classes can be seen.

3.3.3 Precipitation type

One forward scatter type instrument and two disdrometers are partly available for the determination of the precipitation type. Figure 6 shows a histogram displaying the number of events with different precipitation types and temperatures as observed from the Vaisala PWD 21 (forward scatter type instrument, Vaisala Oyj, Finland).

The data include snow events between +5 and $-17\,^{\circ}\mathrm{C}$, with a maximum at $-1\,^{\circ}\mathrm{C}$ and a second smaller maximum around $-15\,^{\circ}\mathrm{C}$. Rain is reported at temperatures down to $-1\,^{\circ}\mathrm{C}$ and mixed precipitation is observed between -1 and $5\,^{\circ}\mathrm{C}$.

A closer look at the snow events (as determined by the Vaisala PWD, not shown) reveals that a robust and consistent result is not possible without further information. The temperature data set and the data from the disdrometer type instruments (where available) suggest that a significant amount of the detected snow events are rather rain events.

This study does not use the precipitation type information further for the development of the adjustment equation. Beside the need for improving the reliability, these data are
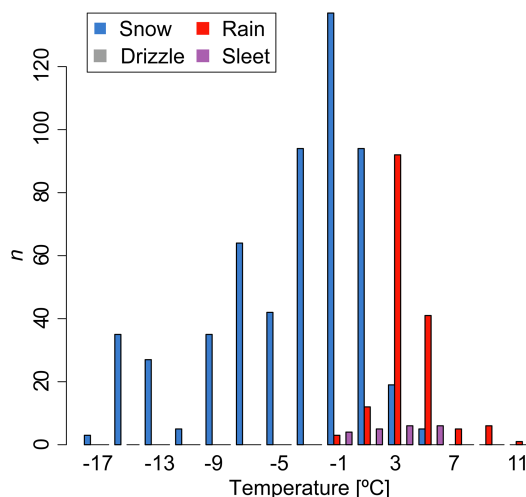

Figure 6. Number of events with different precipitation types and temperatures. Precipitation type is measured by a forward scatter type instrument (Vaisala PWD 21). Event data from 2011–2012 are shown.

presently not available for the majority of the Norwegian standard weather stations.

Further analysis of these data and an optimized use of the instruments and their capacities in order to determine the precipitation type will be performed in the framework of WMO-SPICE.

3.3.4 Precipitation intensity

Based on the observed intensity of the precipitation events a simple analysis has been performed to detect any dependency of the catch ratio on the precipitation intensity. No significant influence of the precipitation intensity can be identified.

3.4 Quantitative analysis

The qualitative analysis indicates a clear temperature dependence of the catch ratio and a non-linear relationship on the wind speed. Precipitation events which are clearly identified as rain or dry snow show two very different catch ratio relationships. It is, however, desirable to develop only one transfer equation considering a continuous transfer from dry snow over mixed precipitation to rain based on data available at standard weather stations: precipitation, wind and temperature.

3.4.1 Existing adjustment functions used in Norway

The literature on the mechanistic relationship between true and measured solid precipitation, given other determinants, is quite scant. Most studies propose relationships that are, to a large extent, empirical, and probably not generic. Førland et al. (1996) suggested the most widely used set of transfer functions for Geonor gauges in cold climate used in the

Nordic countries. The solid form formula has the form

$$p_\text{T} = p_\text{M} g_1(V, T) = p_\text{M} e^{(b_0 + b_1 V + b_2 T + b_3 V T)}, \tag{1}$$

where p_T is true precipitation, p_M is measured precipitation, T is air temperature, V is wind speed at gauge height and (b_0, b_1, b_2, b_3) are parameters. In the same report a related relationship for liquid precipitation is presented:

$$p_\text{T} = p_\text{M} g_2(V, T) = p_\text{M} e^{[c_0 + c_1 V + c_2 \log(I) + b_3 V \log(I)]}, \tag{2}$$

where I is intensity, which in most practical applications must be approximated by p_M. If the exponents in Eqs. (1) and (2) become negative, it is set to zero (no adjustment).

The criteria for using the different transfer functions for the different precipitation types are dependent on temperature:

$$p_\text{T} = \begin{cases} p_\text{M} g_1(V, T) & T \le 0.0°\text{C} \\ p_\text{M} \{g_1(V, T) + g_2(V, I)\}/2 & 0.0 < T \le 2.0°\text{C} \\ p_\text{M} g_2(V, I) & T > 2.0°\text{C}. \end{cases} \tag{3}$$

One immediate criticism of the aforementioned framework of formulae is the lack of continuity between segments when the temperature varies over the limits during an event. Furthermore, the limit criteria in Eq. (3) also exclude the possibility of solid precipitation when the temperature is above $2\,°\text{C}$. Similarly, it is assumed that liquid or mixed precipitation does not occur in cases where the temperature is below $0\,°\text{C}$.

Equation (2) includes intensity for mixed and liquid precipitation. Especially during summer, a wide spectrum of very different precipitation events may occur, also including large differences of typical drop sizes. Therefore, liquid and mixed precipitation catch ratios might be influenced by intensity, which is an indirect measure of drop size. Unfortunately, the true intensity cannot be measured directly since measured precipitation is intrinsically affected by wind-induced loss. The approximation becomes especially inaccurate when the temperature is in the interval where mixed precipitation occurs.

The equations have a validity limited to events with wind speeds lower than $7\,\text{m}\,\text{s}^{-1}$ and temperatures higher than $-12\,°\text{C}$, as no data beyond this range were available at the time of derivation.

3.4.2 Preparative assumptions

Based on: (i) a study of the characteristics of similar data in other studies (e.g. Rasmussen et al., 2012); (ii) consideration of existing adjustment functions (e.g. Goodison et al., 1998); (iii) results from theoretical fluid mechanical studies on rain gauges in wind fields (e.g. Thériault et al., 2012; Nešpor and Sevruk, 1999); (iv) data that are commonly available at a typical meteorological station; and (v) an analysis of the collected data at Haukeliseter during winter, the following attributes of an adjustment function for a given temperature are proposed:

1. The ratio between true and observed precipitation is a function of only wind speed, V.

2. The ratio is monotonically decreasing from unity at $V = 0$ to a limit greater or equal to zero as V approaches infinity.

3. The ratio decreases exponentially as a function of wind speed.

4. The rate of change of ratio varies significantly as a function of wind speed, and can take the value of zero in parts of the domain.

Based on these criteria, a natural choice is a version of Eq. (1) which is non-linear in logarithmic space for a given temperature:

$$R|T = \frac{p_\text{M}}{p_\text{T}} = (1 - \tau) e^{-\left(\frac{V}{\theta}\right)^\beta} + \tau, \tag{4}$$

where $\phi = (\tau, \beta, \theta)$ is the vector of parameters dictating the shape of the relationship.

Equation (4) can be characterized as a bell function, and is generally able to emulate monotonically decreasing functions in the first quadrant. The derivation $\mathrm{d}R/\mathrm{d}V$ approaches zero in the two endpoints for $\beta > 1$ (which is assumed to be the case), and can have this property in a large part of the actual domain, if necessary.

Furthermore, it is assumed that each of the characteristics of Eq. (4) can vary with temperature. But for each property we also consider whether it might be constant for all temperatures. Generally, this can be achieved by formulating the three parameters as functions of temperature, i.e.

$$R = f(V, T) = [1 - \tau(T)] e^{-\left[\frac{V}{\theta(T)}\right]^{\beta(T)}} + \tau(T). \tag{5}$$

The next intuitive question would be: what are the plausible characteristics of the parameter functions $\phi(T)$? An immediate assumption is that the value of the parameters goes from one limit to another when the temperature increases/decreases. Next, it is proposed that the rate of change is at its greatest when the temperature passes through the transition area from dry snow to mixed precipitation. This assumption implies that the parameter functions reach stable values as the temperature moves away from the phase-shift area. These assumptions fit with the pre-analysis of the collected data. They also correspond with Eq. (1).

Furthermore, a continuous transition from dry snow precipitation to mixed precipitation, and perhaps also towards liquid precipitation is needed. In this context, the question of whether intensity could be a significant determinant arises. As this study focuses on winter precipitation only, intensity is assumed to be negligible.

The aforementioned assumptions imply that the parameter functions are well described by sigmoid functions:

$$\phi(T) = \phi_1 + (\phi_2 - \phi_1) \frac{e^{(T - T_\phi)/s_\phi}}{1 + e^{(T - T_\phi)/s_\phi}}. \tag{6}$$
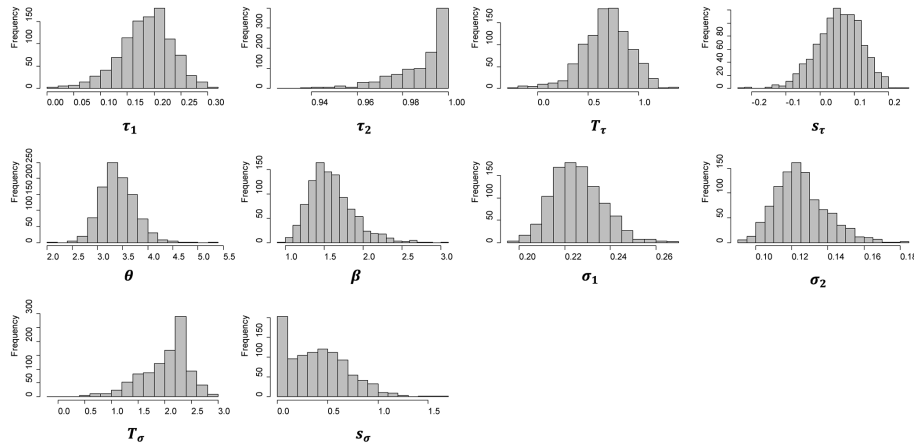
Figure 7. Plots showing the posterior distributions for the parameters in the analysis of the gauge height wind data set.

This type of function has the property of approaching the left limit φ_1 when $T \ll T_\varphi$, and the right limit φ_2 when $T \gg T_\varphi$. The parameter T_φ decides the location of the transition between the two limits, while s_φ dictates the fuzziness of the transition. A small s_φ indicates a rapid change, whereas a large value gives an approximately linear transition. For generality, the number of limits can be increased by using higher-order functions. This study applies only two- and three-level functions. The three-level expressions are constructed using two non-normalized normal distribution functions having the same mode to ensure a continuous transition. Hence this function has a parameter formulating the middle level and two scale parameters determining the fuzziness in the transition between the levels. Mathematically, that can be expressed by

$$\phi(T) = I(T < T_\phi) \left[\phi_1 + (\phi_2 - \phi_1)e^{-\frac{(T-T_\phi)^2}{2 \cdot s_{\phi,1}}} \right]$$
$$+ I(T \geq T_\phi) \left[\phi_3 + (\phi_2 - \phi_3)e^{-\frac{(T-T_\phi)^2}{2 \cdot s_{\phi,2}}} \right]. \quad (7)$$

The letter I symbolizes an indicator function that becomes 0 if the inequality inside the parentheses is false and 1 otherwise. Furthermore, the left- and right-hand limits are given by ϕ_1 and ϕ_3, while the mode of the middle segment is given by ϕ_2.

3.4.3 Statistical inference method

In general, multi-level parameter functions allow for a lot of plausible model forms. A priori, no combination can be ruled out. A statistical model selection method is thus warranted. The Bayesian machinery is attractive in this respect, since it allows the use of prior knowledge. Given a data set D from the Haukeliseter test site that contains $i \in (1, \ldots, n)$ concurrent observations of ratio, wind speed and temperature, a gen-

eral regression is given by

$$R_i = [1 - \tau(T_i)]e^{-\left[\frac{V}{\theta(T_i)}\right]^{\beta(T_i)}} + \tau(T_i) + \sigma(T_i)\varepsilon_i, \quad (8)$$

where ε_i is normally distributed noise with zero expectancy and unity variance and σ is an unknown parameter governing the variance of the measurement error. Considering up to three-level sigmoid functions on each of the four parameters in Eq. (8), this yields 81 possible sub-models. The simplest is of course the one where all parameters are fixed, and the most complex one is where all four parameters are formulated as three-level sigmoid functions. The latter involves 24 unknown parameters that have to be estimated.

Bayesian model likelihood (BML) is used as a model selection tool in this study. In applying BML, it is assured that the simplest possible model is chosen, because the Bayesian model comparison prefers more parsimonious models to more complicated ones (i.e. Jefferys and Berger, 1992). Mathematically, the BML is given by

$$\text{BML}_M \equiv f(D|M) = \int f(D|\underline{\Omega}_M, M) f(\underline{\Omega}_M|M) d\underline{\Omega}_M, \quad (9)$$

where D represents the data set, M denotes one of the 81 possible models, i.e. $M \in (1, \ldots, 81)$, and $\underline{\Omega}_M$ denotes the set of parameters associated with model M. The quantity $f(\underline{\Omega}_M|M)$ is the prior distribution of the parameter set, summarizing our knowledge of what constitutes reasonable parameter values prior to the data. The BMLs give the probability of the data for each proposed model. Those can be used for producing model probabilities or be compared directly between models. In this study, the latter approach is used. The integral in Eq. (9) cannot be evaluated analytically. Therefore numerical methods have to be used. This study applies an importance-sampling technique described in Reitan and Petersen-Øverleir (2009) where it was used to select segmentation models in hydraulic rating curve analysis.

For each model, Bayesian methods are used for evaluating the model parameters. The posterior distributions of the

Table 1. Estimated parameters for the adjustment function, Eq. (10), and the standard deviation of the regression noise, Eq. (11), for three data sets. Each parameter is represented with three values: upper and lower 95 % confidence interval and the best estimate in the middle (in bold type). The parameters for Eq. (10) are shown in (a), whereas the parameters for Eq. (11) are shown in (b).

(a)

	θ	β	τ_1	τ_2	T_τ	s_τ
Gauge height wind data set	(2.89, **3.41**, 4.18)	(1.19, **1.58**, 2.20)	(0.10, **0.18**, 0.27)	(0.96, **0.99**, 1.00)	(0.29, **0.69**, 1.09)	(0.89, **1.15**, 1.50)
10 m wind data set	(4.02, **4.24**, 4.48)	(1.62, **1.81**, 2.03)	(0.14, **0.18**, 0.22)	(0.98, **0.99**, 1.00)	(0.48, **0.66**, 0.84)	(0.93, **1.07**, 1.21)
Gauge height wind data set (unfiltered)	(3.57, **4.55**, 5.75)	(1.05, **1.43**, 1.87)	(0.26, **0.36**, 0.43)	(0.97, 0.99, 1.00)	(0.94, **1.14**, 1.32)	(0.30, **0.44**, 1.60)

(b)

	σ_1	σ_2	T_σ	s_σ
Gauge height wind data set	(0.21, **0.23**, 0.25)	(0.10, **0.13**, 0.16)	(1.17, **2.03**, 2.74)	(0.02, **0.40**, 1.04)
10 m wind data set	(0.17, **0.18**, 0.19)	(0.09, **0.11**, 0.12)	(2.16, **2.35**, 2.83)	(0.00, **0.12**, 0.42)

parameters express the knowledge concerning the parameters after analysing the data. They are numerically calculated from the prior distribution and the likelihood, Eq. (8), using a MCMC (Markov chain Monte Carlo) scheme. The algorithm is based on a relatively general random walk Metropolis algorithm along with an adaptive burn-in routine and a parallel tempering approach (Chib and Greenberg, 2001). More details on Bayesian data analysis and methods are given in textbooks such as by Gelman et al. (2013).

The overall distribution for the parameter set is constructed by assuming prior independence for each parameter $\mathrm{logit}(\tau)$, $\log(\theta)$, $\log(\beta)$ and $\log(\sigma)$. The logit function $\mathrm{logit}(\tau) = \log(\tau/(1-\tau))$ is used in order to restrict τ to be a number between 0 and 1. The aforementioned reparametrization assumes that all parameters are positive a priori. All parameters take values from $-\infty$ to $+\infty$ in logarithmic space. A mathematically tractable and also plausible assumption of normal prior distributions can then be made, presupposing that the parameters are statistically independent a priori. All priors are given mean 0 and standard deviation 10. This constitutes a set of very wide priors that allows for both very small and very large parameter values on the original scale. The reason for this is to avoid the effect of prior information in the subsequent model choice procedure.

The three favoured models from this initial run are chosen and fine-tuned in a second step, in which information from other data sets (i.e. Rasmussen et al., 2012; Thériault et al., 2012) and parameters of associated estimated adjustment functions (of different form) are used to derive more informative priors. Still, the priors are constructed relatively widely to avoid misspecifications. Normal distributions are used for the transformed parameters with means and the following 95 % credibility intervals; $\theta \in (1, 20)$, $\beta \in (0.25, 5)$, $\sigma \in (0.001, 1)$, $\tau \in (0.001, 0.999)$. For the two-level temperature dependence, more specific priors $\tau_1 \in (0.001, 0.5)$ and $\tau_2 \in (0.5, 0.999)$ are defined, assuming an asymptotic limit for R as a function of velocity to be larger for high temperatures than for low.

4 Results

The BML analysis quite clearly favours a model with constant θ and β parameters, and two-level sigmoid functions describing the zero-plane displacement parameter τ and the regression noise standard deviation σ. This means that the following regression is considered with the previously described informative prior:

$$R_i = \left[1 - \tau_1 - (\tau_2 - \tau_1) \frac{e^{\left(\frac{T_i - T_\tau}{s_\tau}\right)}}{1 + e^{\left(\frac{T_i - T_\tau}{s_\tau}\right)}} \right] e^{-\left(\frac{V_i}{\theta}\right)^\beta}$$
$$+ \tau_1 + (\tau_2 - \tau_1) \frac{e^{\left(\frac{T_i - T_\tau}{s_\tau}\right)}}{1 + e^{\left(\frac{T_i - T_\tau}{s_\tau}\right)}} + \sigma(T_i)\,\varepsilon_i, \tag{10}$$

where the associated standard deviation of the regression noise is given by

$$\sigma(T_i) = \sigma_1 + (\sigma_2 - \sigma_1) \frac{e^{(T_i - T_\sigma)/s_\sigma}}{1 + e^{(T_i - T_\sigma)/s_\sigma}}. \tag{11}$$

Equation (11), describing the noise, shows some signs of unequal noise variance when plotted against true precipitation.

The posterior results in the form of histograms of MCMC samples are shown in Fig. 7. Parameter estimates, in the form of the means of the marginal posterior distributions, along with associated 95 % credibility intervals, are displayed in Table 1a and b. The posterior distributions are much narrower than the corresponding prior distributions, suggesting that the choice of prior has little influence on the parameter estimates. The posteriors show little sign of complexities like multimodality and heavy tails. Further, the parameters, which are invariant of the height of the wind speed measurements ($\tau_1, \tau_2, T_\tau, s_\tau$), do not show any practical difference. Performing the same analysis with an unfiltered data set, however, shows a noticeable difference in these parameters, implying that the filtering of the data is a justifiable procedure. The posterior results of that analysis are also listed in Table 1.
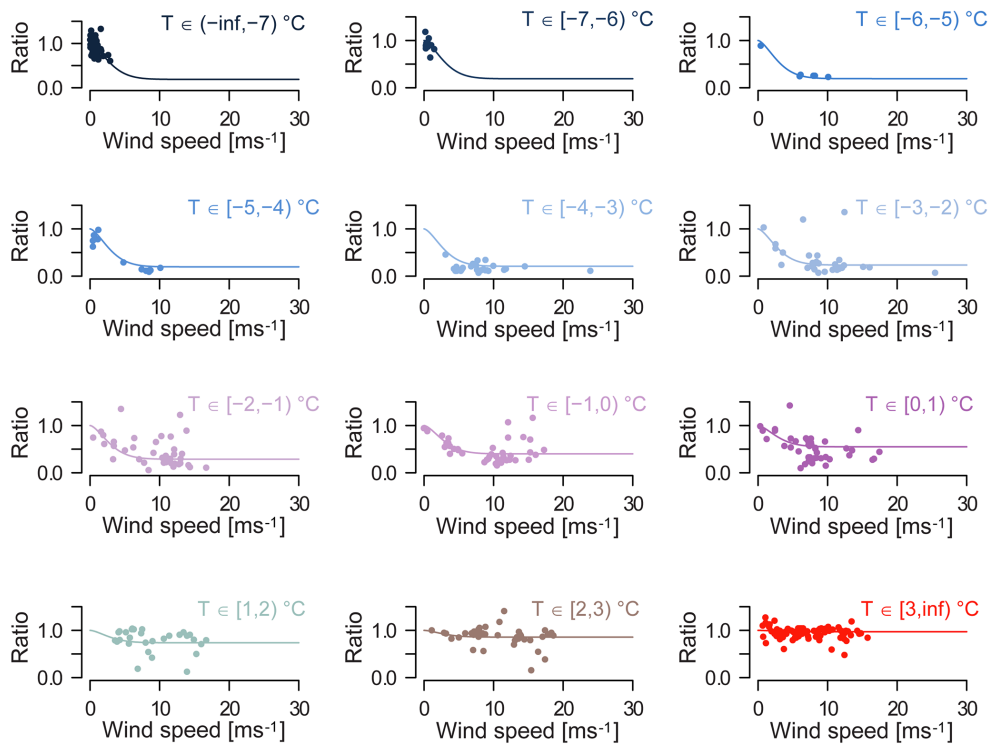
Figure 8. Adjustment function for wind in gauge height for various temperature classes. Adjustment function is calculated with the mean temperature of the individual classes.
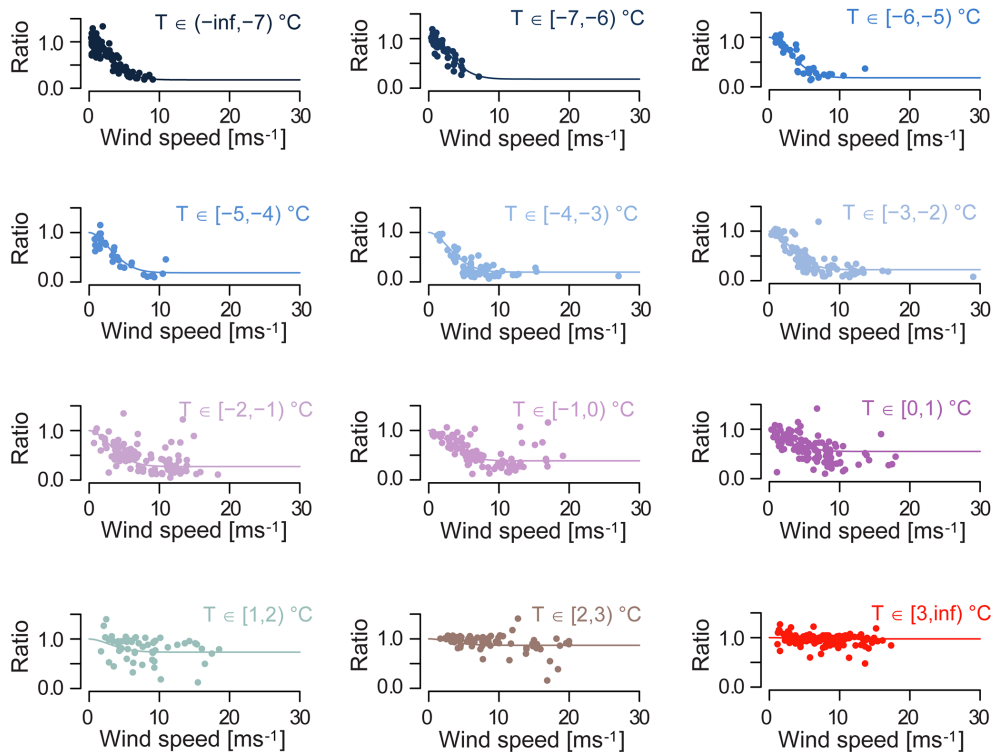

Figure 9. Adjustment function for wind in 10 m for various temperature classes. Adjustment function is calculated with the mean temperature of the individual classes.

As expected, both parameters (θ and β) seem to increase as a function of wind speed measurement height. Finally, the analysis with 10 m wind speed data yields a higher BML than the analysis using wind speed measured at gauge height. This fact indicates that the Bayesian analysis favours the 10 m wind speed data set for the chosen model form. A possible reason might be the better data quality of the 10 m wind speed measurements than of the gauge height measurements despite the applied filtering. In any case, the adjustment functions (ignoring the noise term) are explicitly given by

$$p_{\mathrm{T}} = p_{\mathrm{M}} \left\{ \left[0.82 - \frac{0.81 e^{\left(\frac{T-0.69}{1.15}\right)}}{1 + e^{\left(\frac{T-0.69}{1.15}\right)}} \right] e^{-\left(\frac{V}{3.41}\right)^{1.58}} \right.$$
$$\left. + \frac{0.81 e^{\left(\frac{T-0.69}{1.15}\right)}}{1 + e^{\left(\frac{T-0.69}{1.15}\right)}} + 0.18 \right\}^{-1} \tag{12}$$

for wind speed measured at gauge height and

$$p_{\mathrm{T}} = p_{\mathrm{M}} \left\{ \left[0.82 - \frac{0.81 e^{\left(\frac{T-0.66}{1.07}\right)}}{1 + e^{\left(\frac{T-0.66}{1.07}\right)}} \right] e^{-\left(\frac{V}{4.24}\right)^{1.81}} \right.$$
$$\left. + \frac{0.81 e^{\left(\frac{T-0.66}{1.07}\right)}}{1 + e^{\left(\frac{T-0.69}{1.07}\right)}} + 0.18 \right\}^{-1} \tag{13}$$

for wind speed measured at 10 m.

The results for both adjustment equations are shown in Figs. 8 and 9, respectively.

4.1 Analysis of residuals

How well the derived function and associated covariates described the actual catch ratio is evaluated by analysing the residuals. Standardized residuals, which are the original residuals normalized to have zero expectation and unit variances, are plotted in Fig. 10.

No signs of model misspecification can be seen for the wind speed and temperature covariates. Plotting the residuals against the true precipitation, measured in the DFIR, yields a trumpet shape, which may indicate that the noise variance is dependent on the amount of true precipitation. The panel showing the theoretical quantiles of a normal distribution versus the actual sample quantiles reveals that the residuals have a heavier tail than a normal distribution, which also indicates a non-sufficient description of the noise or uncertainty of the adjusted values.

5 Discussion and outlook

Three winters with precipitation data have been collected and analysed during the study. Precipitation events are identified and afterwards filtered in order to pick only those events
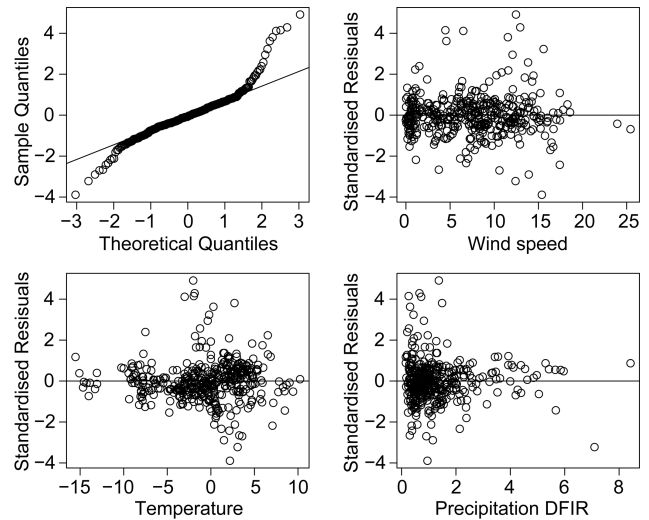

Figure 10. Standardized residuals, which are the raw residuals divided by their estimated standard deviation (bottom and top right) versus wind speed (upper right), temperature (lower left) and precipitation amount (lower right). In the upper left panel the theoretical percentiles from the standard normal distribution are plotted versus the empirical percentiles from the standardized residual distribution.

which are not disturbed by not-controllable parameters, such as for example compromised wind measurements. The classification of the data set using key parameters that possibly influence precipitation loss gives a good idea of the shape of possible adjustment functions. Bayesian statistics are then used to more objectively choose the model describing the data set best. The derived adjustment function depends only on wind speed and air temperature. It calculates the catchment efficiency of a Geonor with Alter windshield compared to a Geonor inside a double fence construction.

It needs to be mentioned that also a DF-shielded precipitation gauge experiences a wind loss. A bush gauge – a precipitation gauge surrounded by equally distributed bushes of similar height – is generally regarded as the best method to measure true precipitation (Goodison et al., 1998). Yang (2014) presents transfer functions between precipitation data from a DFIR to a bush gauge. For lower wind speeds, these relationships suggests that the DFIR catch is very close to true snowfall for the low winds, and about 93 % of "true snowfall" for wind speeds up to 6–7 m s^{-1}. However, the transfer functions by Yang (2014) are only valid for wind speeds below 9 m s^{-1} as no data for higher wind speeds exist. Therefore, no further adjustments are performed in this study.

5.1 Representativeness

The precipitation events from 13 effective measurement months contain a large range of event average wind speeds. For the first time, an adjustment function can be derived from

a sufficient number of events with wind speeds larger than $7–9\,\mathrm{m\,s^{-1}}$. The derived transfer function is valid for event average wind speeds up to $15–20\,\mathrm{m\,s^{-1}}$, which occurred frequently at Haukeliseter. The data clearly support the assumption of a stabilization of the precipitation loss for higher wind speeds. It seems therefore possible to apply the transfer function for even higher wind speeds, since an extrapolation beyond the area of validity does not change the catchment efficiency any further.

In this study, wind speed is measured with sensors mounted at 10 m height (WMO standard) as well as at gauge height (4.5 m for all gauges). As described in Sect. 3.1.2, gauge height wind measurements are partly affected by nearby installations and only unaffected measurements are used for the analysis. Both data sets are used and two different versions of the adjustment function are determined, to be used with 10 m or gauge height wind, respectively. The resulting adjusted precipitation amounts, calculated with either version of the transfer function, agree extremely well. That might be different for gauges at another installation height. A lower gauge height, for example, would result in a larger difference between 10 m and gauge height winds. The use of wind data at gauge height is therefore recommended wherever possible.

The developed adjustment function is solely based on winter data. Nevertheless, quite mild events are also part of the analysis (up to ca. 6–7 °C monthly average temperature), thus covering all three major precipitation types: snow, mixed precipitation and rain. The results for the analysed warmer rain events are very clear and consistent. Summer precipitation, however, is typically characterized by a larger variety of rain types, covering very light long-lasting drizzle to heavy rain or hail showers. That might create quite different precipitation intensities than those observed during this study. An application for temperatures larger than 3 °C is therefore not recommended, until studies evaluating explicitly summer precipitation are available.

Non-systematic scatter can be reduced significantly by means of relevant filters before the Bayesian statistic is applied. The necessity of this method can be confirmed by trying to retrieve the adjustment function based on the unfiltered data set. Some of the derived parameters defining the adjustment function are significantly different and less able to reproduce the real data set. The catch ratios at higher wind speeds, for example, stabilized at a higher value than the adjustment functions based on the filtered data sets suggest.

The scatter, however, is not eliminated completely. The catch efficiency still varies for individual events, especially for mixed precipitation events. Consequently, the resulting adjustment function does not correct the measured precipitation amount perfectly, i.e. adjusting individual events can result in over- or underestimation of the true amounts. An application of the adjustment functions over a longer period, however, should balance out these errors.

Precipitation data sets from operational stations can contain accumulation records not related to precipitation. Wind measurements from wind sensors which are not adequately mounted might lack the necessary quality for a successful use of the adjustment function. This study shows the importance of an extensive quality control of the observations before the application of the adjustment function.

As a matter of course, trace events, i.e. with non-measurable precipitation, cannot be corrected by the presented function. During the course of this study about 5 % of the recorded events (compared to measurements inside the DF) at Haukeliseter showed no significant accumulation in the standard gauges outside the DF. The accumulated sum of these events adds up to 10 % of the observed precipitation at Haukeliseter. These values depend highly on the local climate and are probably very site specific; they may add up to a considerable amount. When correcting precipitation data from a climate perspective, a separate consideration of these trace amounts is necessary, as for example done by Mekis and Vincent (2011).

In Norway, as well as in other countries, the most usual reporting interval at automated weather stations is 1 hour and the adjustment functions are optimized for that time interval. Historically, larger time intervals (12 and 24 h) are widely used. The adjustment function has been applied, successfully, for these longer time intervals for the available data from Haukeliseter in preliminary tests. The length of the precipitation events does not, of course, always match the longer time periods represented by the average wind speed and temperature observations. Precipitation might occur at temperatures and wind speeds quite different from the averages and thus larger uncertainties have to be taken into account when correcting the precipitation loss.

The precipitation event averages of both temperature and wind speed in the present data set cover the climate variations commonly expected in the Norwegian mountains, suggesting that the presented adjustment functions can also be applied to data from other Norwegian sites. However, the influence of other parameters, such as humidity or pressure, has not been studied and no systematic evaluation of the adjustment functions with data from other sites has been performed yet. It is therefore not known to what extent the present adjustment study is valid for sites in other climates and at other altitudes. The co-operation within WMO SPICE, with 20 sites in very different climates, will help to answer this question.

5.2 Comparison with former model

The new adjustment function is based on sufficient data covering low and high wind speeds, thus allowing an extension of the validity beyond $7\,\mathrm{m\,s^{-1}}$ up to $15–20\,\mathrm{m\,s^{-1}}$. Furthermore, it is suitable for all precipitation types, hence avoiding discontinuities resulting from the use of different equations for each phase. Comparisons with the old equation set by Førland et al. (1996) do not show significant differences for
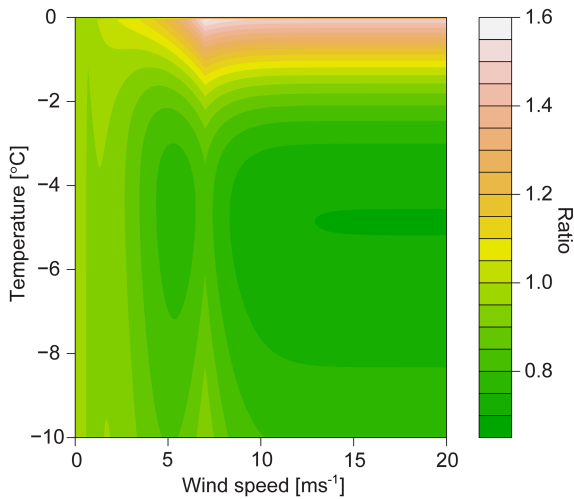
Figure 11. Contour plot showing the ratio between the former and commonly applied correction factor of Førland et al. (1996) and the correction factor presented in this paper. The correction factor is the factor which needs to be applied to the measured precipitation to obtain the true precipitation. Contours higher than one indicate that the method of Førland et al. (1996) gives more precipitation than the new adjustment equation. Note that the analysis by Førland et al. (1996) sets wind speeds above 7 to 7 m s^{-1}.

the adjustment of snow events for wind speeds lower than 7 m s^{-1} and well below O °C. It can easily be seen that the old equation quickly approaches zero as the wind speed grows beyond 7 m s^{-1}, yielding unrealistically large amounts of precipitation. A truncation, where wind speeds above 7 m s^{-1} are set to 7 m s^{-1}, is therefore commonly applied in Norway. Even then, the framework by Førland et al. (1996) differs significantly from the one presented in this study. Figure 11 shows that, for temperatures close to 0 °C and wind speeds above 7 m s^{-1}, the truncated version of the old equation adjusts up to 50 % more precipitation than the new one. This overcorrection is still present for wind speeds below 7 m s^{-1} and decreases with further decreasing wind speeds. A comparison for temperatures above zero is not performed since this involves a third determinant, intensity, in the old correction method.

It should be mentioned that the results from Førland et al. (1996) are based on a manual reference, with a Tretyakov gauge inside the DF. The aerodynamical characteristics of a Tretyakov are surely different from those of a Geonor/Alter shield configuration as used in this study. However, it can be assumed that the effect of the double fence around these different gauges will dominate the overall aerodynamics of the reference system. Therefore, no large deviations are expected. The possible effect of this difference will probably be quantified during SPICE using data from those sites, which are equipped with both references.
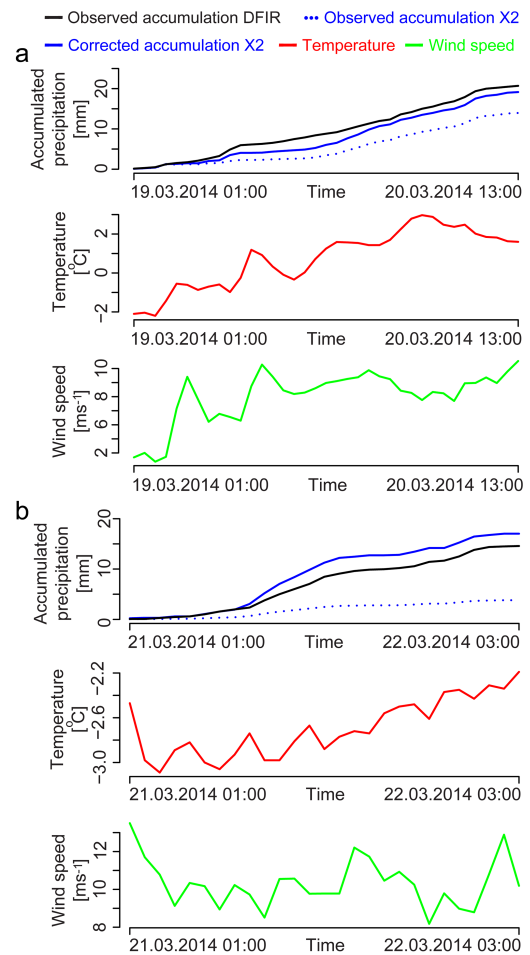

Figure 12. Observed and adjusted accumulation from two precipitation events (**a** and **b**), compared to the accumulation observed in the reference gauge (inside DFIR). Temperature and wind speed during the events are shown in the middle and lower panel, respectively.

5.3 Regression noise and uncertainty analysis

As seen in the residual analysis, the regression noise is not optimally described with Eq. (11). There are quite clear indications of heteroscedasticity in the residuals for increasing true precipitation. Heteroscedasticity is not expected to create any bias, but it does indicate that the uncertainty analysis could be inaccurate. Heavy-tailed residual distributions are also noted. This suggests that the residual distribution belongs to another family than the normal distribution, though symmetric around zero. Uncertainty analysis therefore becomes imprecise and adds to the problems caused by heteroscedasticity.

A further, and perhaps more important, source of inaccuracy is how the regression result is used in this study. It is applied in an inverted form to derive the true precipitation from the ratio. The statistical properties of this quantity, which in the Bayesian formulation is a distribution, are not

Table 2. Precipitation observations from two longer periods and two individual events are adjusted with the presented adjustment function and compared to the data measured by the reference gauge inside the double fence.

Period	Temp (hourly averages)	Wind (hourly averages)	Observed accum. DFIR	Observed accum.	Corrected accum.	Diff. before	Diff. after	Improvement
Mar 2011 30 days	−25 to +5 °C	On average 5–15 m s⁻¹, > 20 m s⁻¹ for some events	78.8	53.2 (X1)	80.5	25.6 (32 %)	−1.7 (−2 %)	30 %
Mar 2012 20 days	−10 to +7 °C	5–25 m s⁻¹	29.3	14.0 (X1)	23.6	15.3 (52 %)	5.7 (20 %)	32 %
19–20 Mar 2014 37 h	−2 to +3 °C	6–13 m s⁻¹	20.7	14.0 (X2)	19.2	6.7 (32 %)	1.5 (7 %)	25 %
21–22 Mar 2014 27 h	< −2 °C	8–15 m s⁻¹	14.6	3.8 (X2)	17.0	10.8 (74 %)	−2.4 (−16 %)	57 %

clear. Adding the fact that the noise is subject to misspecification, makes uncertainty analysis about the true precipitation estimate substantially unreliable at this stage.

While it may be sensible to model the distributional properties of the measured precipitation as a function of wind speed, temperature and the true precipitation, the objective is to use this to predict true precipitation given wind speed, temperature and measured precipitation, as formulated in Eqs. (12) and (13). These formulae however, only relate to estimates of R and the measured precipitation, and do not consider the distributional aspects. A multivariate model for true and measured precipitation would allow for expressing one as a distribution of the other, whether true or measured precipitation is of interest. It is also worth noting that even with a normally distributed R as the denominator, the resulting distribution will be the rather unfamiliar reciprocal normal distribution, which is heavy-tailed and bimodal. The bimodality might not be a problem as long as we require a positive R, but the tails are so heavy that the expectation is not available, making it difficult to evaluate bias. If a distribution with heavier tails is considered for the noise terms, such as the t-distribution, even more inflated tails can be expected. Medians are however preserved during monotonic transformations, which should make Eqs. (12) and (13) valid as median estimates.

The two aforementioned statistical issues – the distribution of the inversion and specification of the regression noise – are beyond the scope of this study, the main objective of which is to develop an adjustment function for measured precipitation. Further investigations with alternative regression models able to deliver a more reliable framework for the uncertainty analysis are currently in progress.

5.4 Application of the adjustment function

A thorough evaluation of the validity of the adjustment functions and a quantification of the actual improvement of the precipitation data, require a detailed study of a large number of individual events as well as time series of various lengths, and would also include data from other sites. The data sets from the similarly equipped WMO SPICE host sites will form a unique database for this kind of study and parts of it will surely be performed within the SPICE effort.

At the time of writing, only a very limited set of data that could be used for evaluation is available. Most of the data are already used in the derivation, and thus do not constitute an independent data set. Therefore, only a few preliminary results can be shown here to illustrate the effects of an application of the adjustment functions.

The adjustment function is applied to precipitation data from two individual events, representing a snow and a mixed precipitation event, see Fig. 12. In addition, data from two longer periods of time in March 2011 and March 2012 are analysed. The results are summarized in Table 2. In all four cases a significant improvement is achieved. Differences between the adjusted precipitation amount and the reference value (measured inside DFIR) are both positive and negative, which might indicate that the remaining differences are actually representing the uncertainty of the method. For the two cases where the original difference was 32 %, the adjusted precipitation amounts differed by less than ±10 % from the DFIR measurements. The remaining differences after adjustment of the two cases with the larger original differences (52 and 74 %) are 20 and 16 %, respectively.

6 Conclusions

Extensive measurements over three winter seasons have given new insight in under-catch of solid precipitation due to wind. Also, a better understanding of the sources of error for measuring precipitation is gained. The measurements performed at Haukeliseter are unique, given the wide range of wind speeds and snow amounts which have been observed.

Clear differences are seen for precipitation classified as dry snow, mixed precipitation and rain when analysing wind-induced under-catch. The under-catch has a pronounced re-

lation to temperature and a non-linear relation to wind speed. For solid precipitation at $-2\,°C$ or below, only 80 % of the assumed true precipitation is caught at wind speeds of $2\,m\,s^{-1}$, and only 40 % at $5\,m\,s^{-1}$. The slope of the catch ratio then levels off markedly and stabilizes at 20 % at $7–8\,m\,s^{-1}$. This base line level is confirmed with data up to $15–20\,m\,s^{-1}$ and will most likely not change for even higher wind speeds.

This is the first time that under-catch of snow at these very high wind speeds in mountainous areas has been documented with observed data. Previous studies assumed a stabilization of the catch ratio for wind speeds above $7\,m\,s^{-1}$, but have up to now not been able to show this explicitly due to poor data coverage.

Because of the variation in the aerodynamical properties for wet snow and mixed precipitation, the results are less unambiguous at temperatures between -2 to $2\,°C$.

Results for the precipitation events at even higher temperatures, above $2–3\,°C$, and thus rain, show a quite small under-catch, especially for wind speeds below $11\,m\,s^{-1}$.

Based on this broadly based data set, a new adjustment function for winter precipitation measured by an automatic precipitation gauge (Geonor) equipped with a single Alter wind shield, is proposed. By means of Bayesian statistics, the model that best describes the observations is selected. The result is one continuous equation which describes the wind-induced under-catch for snow, mixed precipitation and rain events for wind speeds up to at least $20\,m\,s^{-1}$ and temperatures up to $3\,°C$. Input parameters are wind speed and air temperature, thus allowing for easy application at operational weather stations only equipped with basic sensors.

Analyses show the importance of good data quality for successfully retrieving and applying the adjustment functions. Some of the wind measurements at Haukeliseter can be shown to be highly influenced by nearby installations, which has a negative impact on the analysis. Before installing a less disturbed wind sensor at gauge height, a significant amount of data had to be rejected for the analysis. It is therefore highly recommended to use only wind measurements from sensors installed separately and undisturbed when applying the adjustment functions on precipitation measurements.

In this study, the adjustment function is developed for hourly precipitation measurements. However, first tests of the function show promising results for 12 and 24 h measurements as well.

Residual analysis of the adjustment function does not reveal any signs of misspecifications of the chosen model. The accompanying noise model, however, seems unable to adequately describe the uncertainty of the adjustment and requires further investigation. Preliminary analysis suggests that an improvement of the noise model will be possible without changes in the adjustment function itself.

Besides its original purpose, the study site is also a host site for WMO-SPICE. Furthermore, the Norwegian Meteorological Institute will operate the DFIR at Haukeliseter as a long-term reference to monitor the changes in precipitation amount in Norway. The station is also part of an increasing network for supporting improved avalanche forecasting in Norway.

References

Barnett, T. P., Adam, J. C., and Lettenmaier, D. P.: Potential impacts of a warming climate on water availability in snow-dominated regions, Nature, 438, 303–309, 2005.

Bindoff, N. L., Stott, P. A., AchutaRao, K. M., Allen, M. R., Gillett, N., Gutzler, D., Hansingo, K., Hegerl, G., Hu, Y., Jain, S., Mokhov, I. I., Overland, J., Perlwitz, J., Sebbari, R., and Zhang, X.: Detection and Attribution of Climate Change: from Global to Regional, in: Climate Change 2013: The Physical Science Basis. Contribution of Working Group I to the Fifth Assessment Report of the Intergovernmental Panel on Climate Change, edited by: Stocker, T. F., Qin, D., Plattner, G.-K., Tignor, M., Allen, S. K.,

Boschung, J., Nauels, A., Xia, Y., Bex, V., and Midgley, P. M., Cambridge University Press, Cambridge, United Kingdom and New York, NY, USA, 867–952, 2013.

Brown, M. J. and Peck, E. L.: Reliability of Precipitation Measurements as Related to Exposure, J. Appl. Meteorol., 1, 203–207, 1962.

Chib, S. and Greenberg, E.: Understanding the Metropolis-Hastings Algorithm, The Am. Stat., 49, 327–335, 2001.

Førland, E. J. and Hanssen-Bauer, I.: Increased precipitation in the Norwegian Arctic: True or False?, Clim. Change, 46, 485–509, 2000.

Førland, E. J., Allerup, P., Dahlström, B., Elomaa, E., Jónsson, T., Madsen, H., Perälä, J., Rissanen, P., Vedin, H., and Vejen, F.: Manual for operational correction of Nordic precipitation data, DNMI report Nr. 24/96, Norwegian Meteorological Institute, Oslo, Norway, 1996.

Gelman, A., Carlin, J. B., Stern, H. S., Dunson, D. B., Vehtari, A., and Rubin, D. B.: Bayesian data analysis, 3rd Edn., Chapman & Hall, USA, 2013.

Goodison, B. E., Louie, P. Y. T., and Yang, D.: WMO solid precipitation measurement intercomparison: Final report. Instruments and Observing Methods Rep. 67, WMO/TD-No. 872, World Meteorological Organization, Geneva, Switzerland, 1998.

Hanssen-Bauer, I., Førland, E. J., and Nordli, P.Ø.: Measured and true precipitation at Svalbard, DNMI report Nr. 31/96, Norwegian Meteorological Institute, Oslo, Norway, 1996.

Jefferys, W. H. and Berger, J. O.: Ockham's Razor and Bayesian Statistics, Am. Sci., 80, 64–72, 1992.

Mekis, É. and Vincent, L. A.: An overview of the second generation adjusted daily precipitation dataset for trend analysis in Canaca, Atmos. Ocean, 2, 163–177, doi:10.1080/07055900.2011.583910, 2011.

Nešpor, V. and Sevruk, B.: Estimation of wind-induced error of rainfall gauge measurements using a numerical simulation, J. Atmos. Ocean Technol., 16, 450–464, 1999.

Nitu, R. and Wong, K.: CIMO survey on national summaries of methods and instruments for solid precipitation measurement at automatic weather stations, Instruments and Observing Methods Report No. 102, WMO/TD-No. 1544, World Meteorological Organization, Geneva, 2010.

Rasmussen, R., Baker, B., Kochendorfer, J., Meyers, T., Landolt, S., Fischer, A. P., Black, J., Thériault, J., Kucera, P., Gochis, D., Smith, C., Nitu, R., Hall, M., Cristanelli, S., and Gutmann, E.: How well are we measuring snow?, B. Am. Meteorol. Soc., 93, 811–829, doi:10.1175/BAMS-D-11-00052.1, 2012.

Reitan, T. and Petersen-Øverleir, A.: Bayesian methods for estimating multi-segmented discharge rating curves, Stoch. Env. Res. Risk A., 23, 627–642, 2009.

Seneviratne, S. I., Nicholls, N., Easterling, D., Goodess, C. M., Kanae, S., Kossin, J., Luo, Y., Marengo, J., McInnes, K., Rahimi, M., Reichstein, M., Sorteberg, A., Vera, C., and Zhang, X.: Changes in climate extremes and their impacts on the natural physical environment, in: Managing the Risks of Extreme Events and Disasters to Advance Climate Change Adaption. A Special Report of Working Groups I and II of the Intergovernmental Panel of Climate Change (IPCC), Cambridge University Press, Cambridge, UK, and New York, NY, USA, 109–230, 2012.

Sevruk, B.: Methods of correction for systematic error in point precipitation measurement for operational use, Operational Hydrology Rep. 21, WMO Rep. 589, 91 pp., Geneva, Switzerland, 1982.

Smith, C. D. and Yang, D.: An assessment of the GEONOR T–200B inside a large octagonal double fence wind shield as an automated reference for the gauge measurement of solid precipitation, in: Proceedings of the 90th AMS Annual Meeting. American Met. Soc., Atlanta, GA, 2010.

Thériault, J. M., Rasmussen, R., Ikeda, K., and Landolt, S.: Dependence of Snow Gauge Collection Efficiency on Snowflake Characteristics, J. Appl. Meteorol. Climatol., 51, 745–762, 2012.

WMO/CIMO: International Organizing Committee for the WMO Solid Precipitation Intercomparison Experiment: Final Report of the Second Session, Boulder, USA, WMO, Geneva, 74 pp., 2012.

Wolff, M., Brækkan, R., Isaksen, K., and Ruud, E.: A new testsite for wind correction of precipitation measurements at a mountain plateau in southern Norway, in: Proceedings of WMO Technical Conference on Meteorological and Environmental Instruments and Methods of Observation (TECO–2010). Instruments and Observing Methods Report No. 104, WMO/TD-No. 1546, World Meteorological Organization, Geneva, 2010.

Wolff, M., Isaksen, K., Brækkan, R., Alfnes, E., Petersen-Øverleir, A., and Ruud, E.: Measurements of wind-induced loss of solid precipitation: description of a Norwegian field study, Hydrol. Res., 44, 35–43, doi:10.2166/nh.2012.166, 2013.

Yang, D.: Double Fence Intercomparison Reference (DFIR) vs. Bush Gauge for "true" snowfall measurement, J. Hydrol., 509, 94–100, doi:10.1016/j.jhydrol.2013.08.052, 2014.

Yang, D., Kane, D., Zhang, Z., Legates, D., and Goodison, B.: Bias corrections of long-term (1973–2004) daily precipitation data over the northern regions, Geophys. Res. Lett., 32, L19501, doi:10.1029/2005GL024057, 2005.